ResearchGate

See discussions, stats, and author profiles for this publication at: https://www.researchgate.net/publication/271924562

Partial hydration of n-alkyl halides at the water-vapor interface: A molecular simulation study with atmospheric implications

ARTICLE *in* THEORETICAL CHEMISTRY ACCOUNTS · MARCH 2014

Impact Factor: 2.23 · DOI: 10.1007/s00214-014-1455-z

CITATION
1

READS
36

4 AUTHORS, INCLUDING:

Alena Habartova
Academy of Sciences of the Czech Republic
8 PUBLICATIONS **12** CITATIONS
SEE PROFILE

Babak Minofar
Center for Nanobiology and Structural Biol…
30 PUBLICATIONS **588** CITATIONS
SEE PROFILE

Martina Roeselova
Academy of Sciences of the Czech Republic
46 PUBLICATIONS **893** CITATIONS
SEE PROFILE

Available from: Babak Minofar
Retrieved on: 25 January 2016

Theor Chem Acc (2014) 133:1455
DOI 10.1007/s00214-014-1455-z

REGULAR ARTICLE

Partial hydration of *n*-alkyl halides at the water–vapor interface: a molecular simulation study with atmospheric implications

Alena Habartová · Anthony Obisesan · Babak Minofar · Martina Roeselová

Received: 14 October 2013 / Accepted: 18 January 2014 / Published online: 1 February 2014
© Springer-Verlag Berlin Heidelberg 2014

Abstract Classical molecular dynamics simulations with a polarizable force field were used to study adsorption of gas-phase alkyl halides to the surface of liquid water and their hydration properties in the interfacial environment. A systematic investigation has been performed for a set of monosubstituted alkyl chlorides, bromides and iodides of the alkyl chain length from one to five carbon atoms ($C_nH_{2n+1}X$, $n = 1$–5, X = Cl, Br, or I). All alkyl halides readily adsorb to the water surface and exhibit a strong preference for interfacial (partial) hydration. When adsorbed, the alkyl halide molecules reside primarily in the outermost region of the water–vapor interface. The (incomplete) hydration shell of the surface-adsorbed methyl halide species is centered on the methyl end of the molecule, with the halogen atom largely exposed and facing away from water into the gas phase. The maximum hydration of the longer-chain alkyl halides is localized around the α-CH_2 group next to the halogen. With an increasing chain length, the alkyl halide molecules align more parallel to the surface. However, ethyl and propyl halides still have the halogen atom rather exposed, pointing almost freely into the gas phase. The behavior of butyl and pentyl halides on the water surface resembles that of alcohols, with the polar region of the CH_2X group interacting with water and the rest of the increasingly nonpolar hydrocarbon chain pointing on average away from water. Consequently, the halogen atom becomes more, albeit not fully, hydrated. The propensity of alkyl halides for the water–vapor interface along with the specific character of the partial hydration of the surface-adsorbed alkyl halides and their preferred interfacial orientation is likely to be of importance for heterogeneous chemical processes, involving alkyl halides adsorbed on the surface of aqueous aerosol droplets or ice particles in the atmosphere.

Keywords Halogenated organics · Haloalkanes · Adsorption · Interfacial solvation · Interfacial partitioning · Surface orientation · Heterogeneous chemistry

Electronic supplementary material The online version of this article (doi:10.1007/s00214-014-1455-z) contains supplementary material, which is available to authorized users.

A. Habartová · A. Obisesan · M. Roeselová (✉)
Institute of Organic Chemistry and Biochemistry, Academy of Sciences of the Czech Republic, Flemingovo nám. 2, 16610 Prague 6, Czech Republic
e-mail: martina.roeselova@uochb.cas.cz

A. Obisesan
Department of Chemistry, California State University Los Angeles, 5151 State University Drive, Los Angeles, CA 90032, USA

B. Minofar
Institute of Nanobiology and Structural Biology, Academy of Sciences of the Czech Republic, Zámek 136, 37333 Nové Hrady, Czech Republic

B. Minofar
Faculty of Science, University of South Bohemia, Branišovská 31, 37005 České Budějovice, Czech Republic

1 Introduction

Halogenated organic compounds are abundant throughout the atmosphere [1–3]. They are emitted from a number of different sources, both biogenic and anthropogenic. The main natural source has been attributed to oceanic origin [4–6], including the coastal marine biota [7] and salt marshes [8, 9]. Terrestrial sources have also been determined [10], and they include biomass burning [11], oxidative degradation of organic matter in soils [12], and

volcanic emissions [13]. In addition, halogenated organics are produced in industry for the use as pesticides, herbicides, insecticides, fungicides, refrigerants, flame retardants and anesthetics [14–18]. Other anthropogenic sources include human-caused biomass burning [19], and gasoline combustion [20]. Of the halogenated organic compounds, small haloalkane species are particularly abundant in the atmosphere and play an important role in atmospheric reactions. Specifically, short-chain alkyl halides, such as methyl chloride (CH_3Cl), methyl bromide (CH_3Br), methyl iodide (CH_3I), ethyl chloride (C_2H_5Cl), ethyl bromide (C_2H_5Br), ethyl iodide (C_2H_5I), as well as 1-propyl iodide (C_3H_7I) and other propyl halides, have been observed in field studies, along with various multi-substituted halomethanes and haloethanes [4, 6, 7, 12, 14, 21–24].

Most of the alkyl halides are relatively short-lived, as they are rapidly oxidized in the troposphere (the primary sink being the reaction with OH radical) or undergo photochemical degradation [1]. For example, CH_3I has an atmospheric lifetime of 1 week [18], the lifetimes of C_2H_5Cl and C_2H_5Br in the troposphere are of the order of 1 month [14]. (Photo)chemical processing of alkyl halides in the troposphere can release free halogen radicals, which then react with hydrocarbons and are involved in the chemistry of tropospheric ozone, odd nitrogen species (NO, NO_2, HNO_3) and odd hydrogen radicals ($HO_x = HO_2 + OH + H$) [14, 25, 26]. Unlike the other alkyl halides, however, CH_3Cl and CH_3Br are not subject to tropospheric removal. Their relatively long tropospheric lifetimes ($\sim$1 year), combined with their large fluxes into the atmosphere, result in significant amounts of these two species reaching the stratosphere, where their halogen atoms, released through photolysis, contribute to ozone depletion [24, 27–29]. Methyl bromide, in particular, has a large ozone-depleting potential, because bromine is about 50 times more effective than chlorine in destroying ozone as it reacts with reservoir chlorine species, freeing the chlorine to react with additional ozone. Methyl bromide is included in the set of substances controlled under the 1987 Montreal Protocol and its production has been subject to an international phaseout [18, 24].

Alkyl halides contribute significantly to the total amount of halogenated organic gases in the atmosphere. Research to determine the distribution and relative magnitudes of natural and anthropogenic fluxes of alkyl halides has led to much progress, however, their sources and sinks are not yet fully clarified and their global budgets remain imbalanced [30–32]. Thus, in addition to further field measurements and atmospheric modeling studies, there is a need for better understanding of the molecular mechanisms that play a role in the complex biogeochemical cycles of alkyl halides on the local as well as global scales.

Naturally, gas-phase chemical reactions are very important in the atmosphere, as are the reactions taking place in the liquid phase—inside aqueous aerosol, cloud and fog droplets or other kinds of atmospheric moisture. Furthermore, aqueous-phase reactions occurring in the oceans, lakes, rivers, etc., greatly affect atmospheric composition and processes. It has been shown, however, that homogeneous, single-phase reactions may not be sufficient in characterizing the complex atmospheric processes, and heterogeneous reactions occurring at the air–water and air–ice interfaces need to be taken into account. The prime example is the heterogeneous reactions on the surfaces of polar stratospheric clouds resulting in the "ozone hole" formation in the Antarctic [33]. (Photo)chemical reactions on aqueous and ice surfaces in the troposphere play an equally important role [1, 34, 35].

As far as alkyl halides are concerned, a number of photochemical reactions have been studied in the gas phase as well as in solution [36–39], in cryogenic matrices [40] and in amorphous solid water [41, 42]. Interaction of haloalkanes with water vapor, formation of alkyl chloride–water complexes and hydrolysis of alkyl halides to the respective alcohols have been investigated theoretically by means of quantum chemical methods [43–46]. Heterogeneous processes involving alkyl halides received considerably less attention. Interaction of methyl chloride (CH_3Cl) with D_2O co-adsorbed on Pd(111) surfaces was studied using femtosecond sum frequency generation spectroscopy [47], photoinduced reaction dynamics of methyl bromide (CH_3Br) and iodide (CH_3I) on MgO(100) was probed by time delayed multi photon ionization mass spectrometry [48], photodissociation dynamics of methyl iodide (CH_3I) adsorbed on amorphous solid water has been investigated using laser resonance-enhanced multiphoton ionization [49], and photochemistry of CD_3Br co-adsorbed with oxygen on Ru(001) was studied by temperature programmed desorption [50]. While these studies provided significant insight into heterogeneous reaction dynamics of alkyl halides, showing for instance the importance of surface adsorption structure and alignment of the alkyl halide molecules, they have focused predominantly on methyl halides, CH_3X, at solid and/or low temperature surfaces, such as surfaces of metals or amorphous solid water.

Alkyl halide species have been observed in the polar regions and at high altitudes, where they can interact with deep-frozen water surfaces. However, a variety of alkyl halides are found in the boundary layer at mid-latitudes [51, 52] where there is significant potential for interfacial chemistry on liquid surfaces of aqueous aerosols, fog and cloud droplets, the open ocean and also on the quasi-liquid layer of ice. Understanding the adsorption, solvation and dynamics of alkyl halides at the surface of liquid water, which can provide vital information for characterizing such

chemical reactions, is therefore as important as on ice or amorphous solid water. Surface-sensitive techniques such as the sum frequency generation spectroscopy are, in principle, well suited for investigation of molecules at aqueous interfaces. However, the relatively weak alkyl halide–water interaction compared to more traditional surface-active species (e.g., alcohols), resulting in significantly lower surface density and higher orientational disorder, makes the detection of surface-adsorbed alkyl halides a challenging task for this method at ambient temperatures [53].

In the absence of experimental data, computational chemistry methods can be a useful tool to learn about alkyl halide–water interactions. Ab initio calculations have been used to study microhydration of methyl chloride, methyl bromide and pentyl chloride in small water clusters [43, 44, 54]. In addition, hydration properties of a few selected chlorinated and brominated haloalkanes at an extended water–vapor interface have been explored using classical and ab initio molecular dynamics (MD) simulations [53–55]. The latter studies, co-authored by some of us, showed for all of the alkyl halides investigated (methyl chloride/bromide, butyl chloride/bromide and pentyl chloride) a strong preference to reside at the water–vapor interface, similar to other small organic molecules and atmospheric gases [56–61]. Both the classical and ab initio MD simulations also showed that the surface-adsorbed methyl chloride and bromide molecules are preferentially oriented with the methyl group toward water. For butyl and pentyl chloride/bromide, due to their longer nonpolar hydrocarbon chain, a parallel alignment at the water surface was found with the hydrocarbon chain pointing on average slightly to the gas phase.

Heterogeneous reactions occurring in interfacial (multiphase) environments often proceed via different mechanisms and/or with different outcomes than chemical reactions of the same reactants in a homogeneous medium (such as in the gas phase or in aqueous solution) [35]. Unlike in the homogeneous phase, where all spatial orientations of a molecule are equally probable, the alignment imposed by the contact of the molecule with a surface is an important aspect of its interfacial chemical reactivity [50, 62, 63]. While in some cases the confining environment of a surface results in photochemical activity that is sensitive to the molecular orientation [50], in other cases the photochemistry of surface-adsorbed species is not significantly different from that of its gas-phase counterpart [64]. In addition, the asymmetric solvation and/or the reduced cage effect of an incomplete solvent shell may enhance certain reaction channels, while suppressing other ones [65–67].

The distinctly different surface orientation of methyl chloride/bromide and their longer-chain counterparts (butyl and pentyl chloride/bromide) observed in the previous computational studies [53, 54] indicates that significant changes in the character of the hydration of the C–X bond occur as one proceeds along the homologous series of alkyl halides. This, in turn, is likely to have consequences for the heterogeneous (photo) chemistry of alkyl halides on aqueous surfaces. While the previous studies were performed only for selected alkyl halide species, it is the aim of the present paper to systematically investigate the interfacial behavior of a series of *n*-alkyl halides (R–X, where X = Cl, Br, or I, and R = C_nH_{2n+1}, n = 1–5), in order to obtain a more complete picture of molecular orientation and hydration structure of alkyl halides, when adsorbed on the surface of liquid water. In addition to a full set of alkyl chlorides and bromides, the current study includes also alkyl iodides, which, to the best of our knowledge, have not been previously investigated as regards their adsorption at the liquid water–vapor interface.

We report results of classical MD simulations in which individual alkyl halide molecules interact with the surface of a liquid water slab at room temperature. The MD trajectories were analyzed in terms of propensity for interfacial solvation, surface residence times, interfacial alignment and hydration shell structure of the surface-adsorbed alkyl halide molecules. The comparison within the set of *n*-alkyl halide species allows us to characterize the trends in interfacial hydration properties of alkyl halides, depending on the type of the halogen substituent and the length of the hydrocarbon chain. The results are discussed in the context of heterogeneous reactions of alkyl halides on atmospheric aqueous-vapor and ice-vapor interfaces.

2 Computational methods

Interaction of alkyl halides with the aqueous surface was studied by classical MD simulations with polarizable force fields. We focused on *n*-alkyl halides with a general formula R–X, where X stands for Cl, Br or I, and R = C_nH_{2n+1}. The number of carbon atoms in the alkyl chain, n, was varied from 1 to 5. In the rest of the paper, the alkyl halide species with the chain length of 1 through 5 carbon atoms will be referred to as MeX, EtX, ProX, BuX, and PenX, X = Cl, Br or I. The simulated systems consisted of 2 (identical) alkyl halide molecules and 863 water molecules, forming a slab of liquid in the central part of the simulation box, with two water–vapor interfaces perpendicular to the z-axis. The x-, y- and z-dimensions of the rectangular parallelepiped simulation box were set to 30.0, 30.0 and 100.0 Å, respectively. Periodic boundary conditions were applied in all three dimensions. The setup of the systems can be seen in Fig. 1, showing typical snapshots from simulations of MeCl through PenCl.

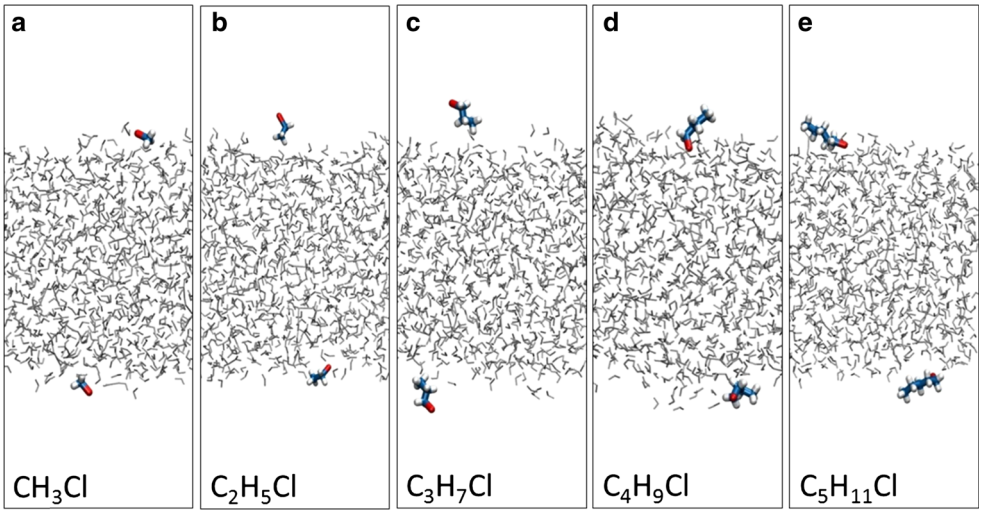

Fig. 1 Examples of the simulated systems showing the water slab placed in the central part of the simulation box and two identical alkyl halide molecules, each at one of the water–vapor interfaces: **a** methyl chloride, **b** ethyl chloride, **c** propyl chloride, **d** butyl chloride and **e** pentyl chloride. Color coding: water—*dark gray*, carbon—*cyan*, hydrogen—*light gray*, chlorine—*red*. The same system setup was employed for alkyl bromides and iodides

The alkyl halide species were modeled using the general amber force field (GAFF) [68], whereas for water molecules the POL3 model [69] was employed. Thus, in addition to the standard Lennard-Jones repulsion and dispersion interactions and the Coulomb forces between the charged sites, description of both water and alkyl halides included an explicit treatment of polarization interaction. This approach has been successfully used in a previous MD study of selected alkyl chlorides and bromides [53] and has been validated by comparison with ab initio structure calculations on alkyl halide–water clusters [43, 44, 54, 70] and ab initio MD of alkyl chlorides on water surface [54]. To obtain partial charges at the atom sites of the alkyl halide molecules, ab initio geometry optimization using the Gaussian 03 package [71] was performed, employing the MP2/cc-pVDZ method. The cc-pVDZ basis set for the iodine atom was downloaded from the Basis Set Exchange web page of the EMSL basis set library [72–74]. The ab initio calculation was followed by the restrained electrostatic potential (RESP) fitting according to the Merz–Singh–Kollman scheme [75] using the Antechamber program [76] of the Amber program package [68, 77]. The optimized geometries, atomic charges and other force field parameters of all alkyl halide molecules considered in this study are summarized in the Supplementary Information.

As the starting configuration for each simulation, two identical alkyl halide molecules were added into the simulation box containing a pre-equilibrated liquid water slab. The alkyl halide molecules were placed in the gas-phase region of the box, approximately 2 Å away from either of the two interfaces. Upon energy minimization, all systems were equilibrated for several hundred picoseconds, followed by a 20 ns production run. The simulations were carried out in the NVT ensemble at 300 K, and the temperature was controlled by the Berendsen thermostat [78] with the coupling constant of 0.05 ps. Equations of motion were integrated using the leap-frog algorithm [79] with a timestep of 1 fs. The short-range nonbonded interactions were truncated to zero beyond the cut-off distance of 12.0 Å, and the long-range part of the electrostatic interactions was accounted for by the particle mesh Ewald method [80, 81]. In the alkyl halide molecules, all bonds involving hydrogen atoms were constrained using the SHAKE algorithm [82], water molecules were kept rigid by SETTLE [83]. Atomic coordinates were sampled for analysis at 5 ps intervals. All simulations were performed employing Amber8 [68] or Amber11 [77] program packages. VMD program was utilized for visualizations [84].

3 Results

Typical results of MD simulations of alkyl halide molecules interacting with a liquid water slab are shown for alkyl chlorides in Fig. 2, where the z-coordinate of the chlorine atom is plotted versus time for a 2 ns segment selected from the 20 ns simulation. The simulations of alkyl bromides and alkyl iodides yielded essentially the same picture and, therefore, are not shown here. In each case, the simulation box contained two (identical) alkyl chloride molecules marked red and green. The center of the slab is set to $z = 0$, the bulk water region is situated approximately between $z = \pm 12$ Å. The two pairs of horizontal dashed lines indicate the approximate location of the two water–vapor interfaces, corresponding to the interval of z-coordinates, in which water density decreases from 90 to 10 % of its bulk value (the so-called "90–10" definition of the liquid–vapor interface). As can be seen from Fig. 2, alkyl chlorides remain most of the time within the interfacial water layer. Visual inspection of the

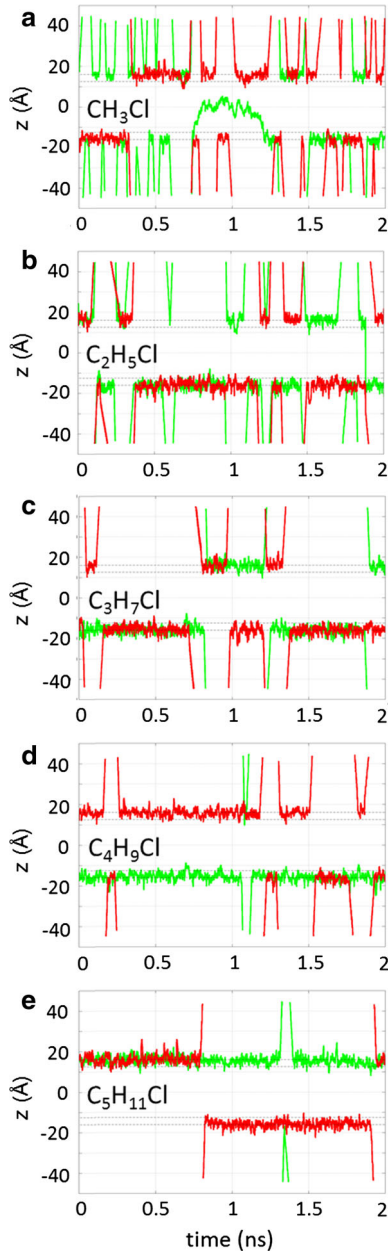

Fig. 2 Trajectories of two identical alkyl chloride molecules interacting with the water slab (one depicted in *red* and the other one in *green*), projected onto the z-coordinate normal to the water–vapor interface: **a** methyl chloride, **b** ethyl chloride, **c** propyl chloride, **d** butyl chloride and **e** pentyl chloride. A 2 ns section of the simulation data is shown in each case. The approximate location of the two water–vapor interfaces of the water slab is indicated by the horizontal dashed lines, $z = 0$ corresponds to the middle of the slab

simulation trajectories reveals that, while adsorbed, the alkyl chloride molecules readily diffuse on the surface of water. They, however, only seldom become fully solvated in the bulk liquid. On the other hand, they frequently undergo desorption into the gas phase. Due to the periodic boundary conditions, if a molecule evaporates from the water surface and leaves the simulation box, it will re-enter the box from the opposite side and impinge onto the other surface of the aqueous slab. A molecule can also diffuse from one interface to the other through the water slab. Thus, both alkyl chloride molecules are sometimes present at the same interface during the simulation, although they mostly remain laterally well-separated and rarely get into the vicinity of each other.

The series of Fig. 2a through e illustrates the effect of the chain length on the behavior of an alkyl chloride molecule. While MeCl did occasionally enter the interior of the water slab and became fully solvated, such episodes were rare and on average shorter with EtCl and ProCl. In the course of the 20 ns trajectory, EtCl exhibited only four absorption events, one of which can be seen in Fig. 2, and a single absorption event of ProCl occurred (not shown in Fig. 2). No uptake of BuCl and PenCl was observed during the entire 20 ns simulations. At the same time, as the alkyl chain gets longer, the volatility of alkyl halides decreases; the molecule spends more time at the surface and its interfacial residence times get (on average) longer. Alkyl bromides and iodides show similar trends, albeit with increasingly longer residence times (from chlorides to bromides to iodides), which can be rationalized in terms of increasing strength of their interaction with the surface of water due to stronger dispersion and induction forces between the larger halogen atoms and water.

To quantify the above trends obtained from the computed MD trajectories, we identified the individual surface residence events and determined their duration for each alkyl halide species. The duration of a residence event was defined as the time continuously spent by a molecule within one of the liquid–vapor interfacial regions of the water slab, i.e., either within the z-coordinate interval from 6 to 25 Å or from −6 to −25 Å. Note that these z-coordinate limits differ from the standard (averaged) "90–10" definition of the water–vapor interface; they were chosen so as to account for fluctuations of the instantaneous position of alkyl halide molecules along the interface normal when adsorbed at the water surface. By assuming first-order kinetics, we obtained a characteristic surface residence time, τ, of each compound as the e-folding lifetime calculated by fitting the residence times distribution to an exponential function $f(t) = A \exp(-t/\tau)$. An example of the analysis of the residence events is shown for MeCl in the Supplementary Information, Figure S1. Results for the full set of alkyl chloride species, obtained using the above described procedure, are summarized in Table 1. The residence times increase systematically with the chain length, from about one or two hundred picoseconds for MeCl and EtCl to about one nanosecond for PenCl. Similar increase by roughly an order of magnitude between the methyl and pentyl species was observed also for alkyl bromides and iodides, albeit their residence times are on average

Table 1 Average residence times of alkyl chlorides at the water–vapor interface (numbers in parenthesis correspond to the 95 % confidence interval)

	CH_3Cl	C_2H_5Cl	C_3H_7Cl	C_4H_9Cl	$C_5H_{11}Cl$
τ (ps)	140 (124,158)	197 (162,250)	535 (437,690)	662 (492,1010)	1007 (684,1915)

Table 2 Average residence times of methyl chloride, methyl bromide and methyl iodide at the water–vapor interface (numbers in parenthesis correspond to the 95 % confidence interval)

	CH_3Cl	CH_3Br	CH_3I
τ (ps)	140 (124,158)	161 (144, 183)	178 (157,205)

somewhat longer with respect to the corresponding alkyl chlorides. The increase of residence times in the series chloride–bromide–iodide is illustrated in Table 2 for the case of methyl halides. However, it should be noted that these calculations were performed to provide only a qualitative picture of the surface residence times and the effects due to the increasing chain length and the size of the halogen. We would like to emphasize that the precision, with which the values of τ were determined (expressed using the 95 % confidence interval in Tables 1 and 2), decreases substantially for the longer-chain species because as the individual residence events get longer with increasing molecular size (and, hence, larger attraction with the water surface), the total number of events within a fixed simulation time drops down dramatically (see Fig. 2). For example, less than 80 residence events were detected for ProCl and only about 20 for PenCl during a 20 ns long simulation, compared to over 200 events for MeCl.

The overall solvation preferences of alkyl halide species at the water–vapor interface can be visualized in terms of the probability distribution (density profile) in the direction normal to the interface. The results are shown in Fig. 3. In each plot, the gray curve corresponds to the density of water that gradually decreases across the water–vapor interfacial region from its constant bulk liquid value to (almost) zero in the vapor phase. The thin dashed horizontal line represents the Gibbs dividing surface (GDS), which is approximated by the position along the z-axis halfway between where the water density is 10 and 90 % of the bulk value. This is to provide a common point of reference for the location of water surface in each system and guide the eye in the figures. The blue curves denote the terminal carbon of the alkyl chain (the CH_3 carbon), and the curves corresponding to the halogen atoms are depicted in orange (Cl), brown (Br) and purple (I). All density

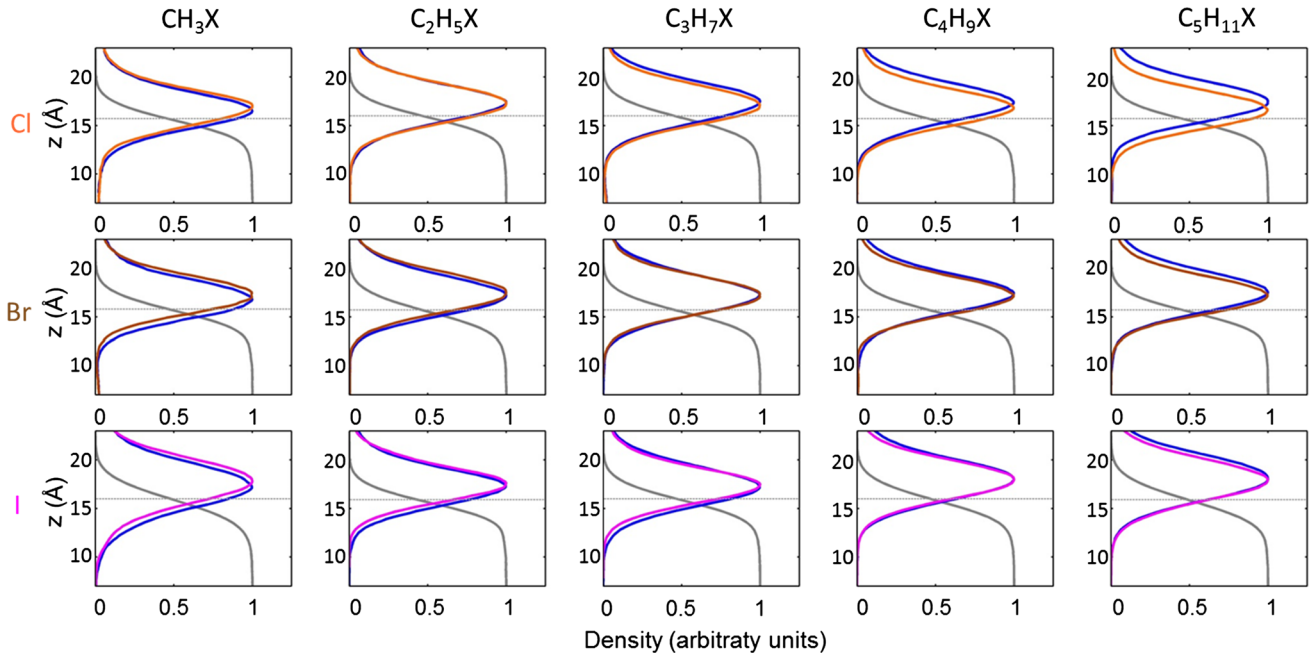

Fig. 3 Density profiles of alkyl halides across the water–vapor interface of the water slab. Color coding: *gray*—water, *blue*—carbon atom of the terminal CH_3 group, *orange*—chlorine, *brown*—bromine, *purple*—iodine. The *horizontal dashed line* denotes the Gibbs dividing surface representing the approximate location of the water–vapor interface. All density profiles were averaged over the two equivalent interfaces, the halogen and carbon profiles were normalized by the corresponding density maximum

profiles were averaged over the two equivalent interfaces and scaled by the respective density maximum.

In Fig. 3, all alkyl halide densities are significantly enhanced in the interfacial region compared to the gas as well as the bulk liquid phases. This corroborates the overall picture obtained from the trajectories (Fig. 2) and demonstrates the propensity of all of the present alkyl halide species for the water–vapor interface. As discussed above, the smaller molecules (especially methyl halides) were observed to occasionally enter the interior of the water slab, albeit only for short periods of time relative to the total length of the simulation. This is reflected in the corresponding density profiles penetrating somewhat deeper into the aqueous phase and having non-zero value in the bulk region of the water slab when compared to the longer-chain species. At the same time, the interaction of all alkyl halides with the water surface is rather weak and, while adsorbed at the surface, they are found predominantly in the outermost region of the aqueous interface. This can be seen from the positions of the density profile maxima, which are all located outside of the GDS. Finally, a non-zero value of density profiles in the gas-phase region, in particular for the smaller alkyl halides, is due to their frequent desorption from the aqueous surface. The above described solvation behavior is characteristic for all of the alkyl halides investigated here, with only minor differences between alkyl chlorides, bromides and iodides.

In addition to the propensity of alkyl halides to reside in the aqueous interfacial region, the density profiles displayed in Fig. 3 also provide information on the preferred molecular orientation of each species at the water surface. This can be inferred from the relative displacement between the density profiles of the halogen atom and the carbon of the CH_3 group in each case. In accord with previous studies [53, 54], the interfacial density peak of the carbon atom of all three methyl halides is shifted toward the interior of water slab relative to the halogen atom, indicating that the methyl halide molecules are oriented with the CH_3 group on average closer to water and with halogen atom pointing to the gas phase. As one proceeds in Fig. 3 along the homologous series for Cl, Br and I, the relative positions of the two density profile curves change. With an increasing chain length, both the curves first overlap, indicating parallel alignment of the molecule with the surface. Eventually, the CH_3 carbon curve moves further away from water relative to the halogen one, as can be seen in the density profiles of the PenX species. This general trend is present in all three alkyl halide series, albeit the details differ somewhat depending on the halogen atom.

To explore the orientation preferences of alkyl halides at the water–vapor interface in more detail, we analyzed the MD trajectories of individual alkyl halide species in terms of the orientation distribution P(cos θ), where θ is the angle between the interface normal (z-axis) and the molecular vector X $\rightarrow$ C(H_3) pointing from the halogen atom X (=Cl, Br, or I) to the carbon atom of the terminal methyl group. (Note that the molecular vector simply connects the two ends of a molecule, while the molecules are flexible and undergo conformational changes during the simulation, as can be seen for instance from the snapshots in Fig. 1). Using this definition, cos $\theta = 0$ means that the molecule is aligned with the molecular vector parallel to the surface, cos $\theta = 1$ corresponds to the molecular vector-oriented perpendicular to the surface with the methyl group pointing to the gas phase, and cos $\theta = -1$ denotes a perpendicular orientation of the molecular vector relative to the surface with the methyl group pointing toward water.

The orientation distributions for the series of alkyl chlorides, from MeCl to PenCl, are plotted in Fig. 4. In agreement with previous studies [53, 54], the results show that the MeCl orientations with the chlorine atom facing the water surface are the least probable, whereas orientations parallel to the interface and, in particular, tilted orientations with the methyl group pointing toward the water surface are preferred. The maximum around cos $\theta = -0.5$ corresponds to a tilt angle of 120 degrees between the MeCl molecular vector and the surface normal. The orientation distribution is, however, rather broad and relatively flat, indicating that the MeCl molecules adsorbed at the water–vapor interface are rotationally highly mobile and sample a large range of orientations with respect to water surface. The P(cos θ) is subject to relatively large uncertainty close to cos $\theta = \pm 1$ due to limited sampling when the angle θ approaches 0 and 180 degrees, therefore, the P(cos θ) values close to cos $\theta = \pm 1$ are less reliable than the "central" part of the distribution. The error of

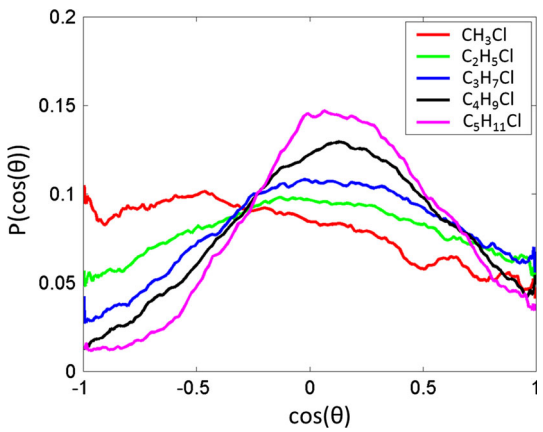

Fig. 4 Orientation distributions of alkyl chlorides at the water–vapor interface. Angle θ is the angle between the interface normal (z-axis) and the molecular vector X $\rightarrow$ C(H_3) pointing from the halogen atom X (=Cl, Br, or I) to the carbon atom of the terminal methyl group

calculated P(cos θ) values, estimated based on block averaging, amounts to ± 0.01 everywhere except for cos θ approaching the limits of the $(-1, 1)$ interval; within the intervals corresponding to $0.9 < |\cos\theta| < 1$, the error of P(cos θ) increases from ± 0.01 to ± 0.03. Nevertheless, even after taking into account the uncertainty in P(cos θ), the preference for the MeCl orientations with the methyl group pointing toward the water surface and the Cl atom toward the gas phase remain statistically significant. (The errors of the P(cos θ) distributions of the rest of the alkyl halide molecules, discussed below, are similar to those given here for MeCl.) With an increasing length of the molecule, the distributions become less broad, which implies gradual reduction of orientational flexibility. At the same time, the distribution maxima shift systematically toward higher cos θ values: While the maxima of EtCl and ProCl distributions are located around cos $\theta \sim 0$, corresponding to parallel alignment of the molecules with the water–vapor interface, the maxima for BuCl and PenCl are found at cos $\theta \sim 0.15$, indicating tilted orientation with the hydrocarbon chain pointing on average slightly away from water at an angle of approx. 10 degrees between the molecular vector and water surface.

Alkyl bromides and iodides follow the same trends as described above for the chlorinated species. The comparison of the orientation distributions of alkyl bromides and iodides with those of alkyl chlorides (see Supplementary Information, Figure S2) shows that alkyl halides of the same chain length exhibit similar behavior (the distributions corresponding to one chain length agree with each other within the statistical uncertainty). Specifically, all methyl halides have a broad distribution of orientations with a maximum corresponding to the methyl group closer to the aqueous phase than the halide end of the molecule, which is more exposed to the vapor phase. The longer-chain molecules, on the other hand, preferably align parallel to the surface, with a slight tendency for the hydrocarbon tail to point away from the aqueous surface. In summary, the orientation analysis thus confirms the conclusions drawn from the density profiles (Fig. 3). We note that the present findings regarding the preferred interfacial orientation of alkyl halides are relevant for individual molecules interacting with water surface, i.e., for the case of low surface number densities. At higher surface coverage (larger number densities), when the alkyl halide molecules get in contact with each other, their mutual interaction may result in re-orientation of some or all of the surface-adsorbed molecules. This concerns in particular the longer-chain alkyl halides that tend to orient more perpendicular to the water surface with increasing surface coverage, albeit to a significantly lesser degree than the corresponding alcohols [53].

The orientation distribution P(cos θ), discussed above, describes molecular orientation with respect to the z-axis perpendicular to both (parallel) global interface planes of the water slab. However, the P(cos θ) distribution does not take into account instantaneous local corrugations of the aqueous surface. In addition, it gives only limited information about hydration of an alkyl halide adsorbate at the local, molecular level. To take into consideration the effect of surface flexibility and to obtain more detailed knowledge about local hydration of alkyl halides at the water–vapor interface, we evaluated the spatial distribution function (SDF) of water around the individual alkyl halides. SDF represents a spatial (3D) histogram of particle number (spatial number density) relative to a central particle. It thus combines information on both radial and angular distribution of solvent molecules around a solute or, as in the present case, an adsorbate.

Figure 5 shows spatial distributions of water oxygen atoms around the surface-adsorbed alkyl halide molecules, averaged over 20 ns simulations. One randomly selected conformation is shown for each alkyl halide species. To construct the spatial density maps, each system configuration (saved at regular intervals along the trajectory) was transformed into a coordinate system having the halide atom X as the origin, the *x*-axis coinciding with the X–C1 bond, the X, C1, and one of the adjacent H atoms defining the *xy*-plane (with the *z*-axis perpendicular to it). The spatial coordinates of all water oxygen atoms were then recorded with respect to this molecule-fixed coordinate system. In this way, positions of water molecules around the alkyl halide molecule are obtained regardless of the instantaneous orientation of the alkyl halide molecule relative to the global water–vapor interface. The distributions plotted in Fig. 5 represent the density isovalue corresponding to 1.5 times the density of bulk water. The SDF plots show that methyl halides have the (incomplete) hydration shell centered on the methyl end of the molecule, leaving the halogen atom fully exposed. For the rest of the species, the maximum hydration is localized around the α-CH_2 group next to the halogen, in accord with the results of ab initio calculations for pentyl chloride [54]. As one proceeds along each of the alkyl halide series, however, there are important differences as regards the hydration of the halogen atom. While in ethyl halides the C–X bond still essentially points away from water, the increasing length—and, hence, hydrophobicity—of the alkyl chain results in gradual re-orientation of the C–X bond relative to the hydration shell, which thereby extends to the vicinity of the halogen. Consequently, ethyl and, to a large degree, also propyl halides have the halogen atom fairly exposed, whereas in butyl and pentyl halides the halogen becomes partially hydrated. The SDF analysis thus supplements the above discussed orientation distributions and provides additional, more specific information on the hydration structure of alkyl halides. In particular, it shows that while

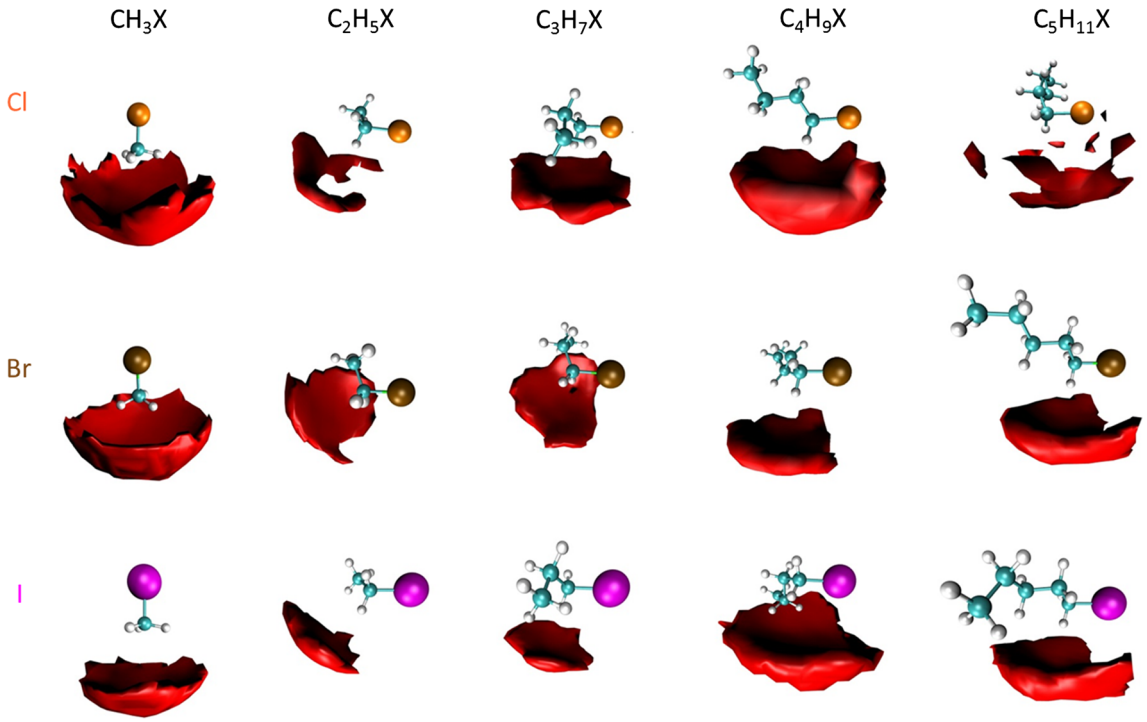

Fig. 5 Spatial density distributions of water around alkyl halide molecules as obtained by averaging over 20 ns MD simulations. Color coding: carbon—*cyan*, hydrogen—*light gray*, chlorine—*orange*, bromine—*brown*, iodine—*purple*. The spatial distributions (*red*) are plotted for the isodensity value of water oxygen corresponding to 1.5 times the density of bulk water

the alkyl halides sample a rather broad range of orientations at the water–vapor interface, sufficient translational and rotational mobility enables the interfacial water molecules to adopt energetically favorable configurations around the surface-adsorbed alkyl halide molecule even if its instantaneous orientation relative to the global water–vapor interface is quite far from optimal.

4 Discussion

The MD simulations of full series of monosubstituted chloro-, bromo- and iodoalkanes with 1–5 carbon atoms in the alkyl chain, the results of which are presented in the preceding section, allow us to identify common features relevant for alkyl halide–water interaction, and to characterize the trends in interfacial hydration properties of alkyl halides, as they change with the type of the halogen atom and the length of the alkyl chain.

While the alkyl halides can be classified as hydrophobic, our results show that they readily adsorb to the water surface. This is in accord with the findings of previous studies [53, 54, 56–59, 61, 85], which indicated that the propensity of gaseous molecules for the water–vapor interface is a generic effect, present for both hydrophobic and hydrophilic species [57]. The underlying reason is the opportunity for the surface-adsorbed molecules to make use of the attractive van der Waals and electrostatic interactions with the aqueous medium without significantly perturbing the hydrogen-bonded network of liquid water. Naturally, the details of the interfacial behavior, such as the extent of surface enhancement or characteristic surface residence times, may differ substantially between different classes of compounds (as well as between individual compounds of the same class), depending on the character and strength of the interaction with water and other molecular properties. The present MD simulations demonstrate that although the interaction of alkyl halides with water is relatively weak, they adsorb to aqueous surfaces and can accumulate in the air–water interfacial region, although they are traditionally not viewed as being "surface active."

In addition to the tendency to preferentially reside at the water–vapor interface, which is common for all of the alkyl halide species investigated here, the MD trajectories also revealed the differences in the interfacial behavior of individual compounds. Methyl halides, being the smallest of the species, are the most volatile and exhibit the shortest surface residence times ($\sim 10^{-10}$ s with the present model). At the same time, they become most easily dissolved in bulk water. With increasing molecular mass within each of the chloro-, bromo-, and iodoalkane series, the molecules get increasingly confined to the interfacial region, as they desorb less frequently into the gas phase and

do not enter the bulk liquid phase. Consequently, the surface residence times grow by about an order of magnitude (to $\sim 10^{-9}$ s) between methyl and pentyl halides. The effect of the halogen atom is less pronounced: The behavior of the compounds of the same chain length, but with a different halogen substituent, is rather similar, with only a moderate increase of the residence times from the alkyl chloride to the corresponding alkyl bromide and iodide.

The above discussed properties and trends are in agreement with low solubility [86] and relatively small Henry's law constants [87] of alkyl halides, and agree well also with the changes in solubility and Henry's law constant along the homologous series of *n*-alkyl halides (see Supplementary Information). This gives us confidence that qualitatively the present MD simulations provide a reliable picture of alkyl halide solvation in aqueous interfacial environment. The quantitative results, such as the precise values of the residence times (Tables 1, 2) or the exact details of the liquid phase—interface—gas-phase partitioning (Figs. 2, 3), depend to a certain degree on the specific model employed in the MD simulations. In particular, the present model was not optimized to reproduce the hydration free energy of the alkyl halide species. This leads to underestimation of the strength of the alkyl halide–water interactions and, thus, of the magnitude of the surface effect, as shown in our recent study for methyl chloride [55]. The results can, therefore, be viewed as a lower estimate of the surface residence times and the interfacial preference of the alkyl halide investigated. At the same time, since polarization interaction is explicitly included in the current model, the model is likely to provide a reliable description of the asymmetric hydration of alkyl halides in the interfacial aqueous environment [56, 88].

The propensity of a compound for the air–water interface becomes important in systems with large interface area. In atmospheric chemistry, the most typical case, in which the air–water interface often dominates, is water droplets dispersed in air (as cloud and fog droplets, dew and mist). Another example is air bubbles dispersed in ocean water, the bursting of which gives rise to aqueous aerosol. While water droplets play a crucial role in scavenging organic compounds from the air, air bubbles can transport dissolved organics to the ocean surface, where the organics are further transferred to the aerosol phase. In the above systems, characterized by one phase (liquid or gas) dispersed in another (bulk) phase, the conventional approach based on the bulk phase gas–liquid partitioning (e.g., the Henry's law) is insufficient. In such cases, the surface has to be taken into account, as surface adsorption can affect the mass transfer across the interface, and reactions at the interface between the two phases may become significant.

The results of the present study, showing interfacial enhancement for a large set of alkyl halides, indicate that partitioning to the interface—in addition to the partitioning between the air and the droplet (bulk liquid) phase—may need to be included to correctly describe the uptake of gas-phase alkyl halides into aqueous droplets dispersed in air. While experimental and/or modeling studies of uptake by aqueous droplets are missing for alkyl halides, the importance of the interface partitioning of these compounds has been demonstrated in the field of water treatment, in separation processes using minute air bubbles to remove pollutants from water by surface adsorption. Experimental and mathematical modeling of the bubble columns has shown that the mass transfer rate of alkyl halides from the aqueous phase to air bubbles as well as the adsorption capacity of the air bubbles for alkyl halides increased with decreasing size of the air bubbles [89–91]. Similar mechanisms are thus likely to play a role also in the behavior of alkyl halides toward wet deposition (uptake by dispersed aqueous droplets) in the atmosphere.

As far as the reactivity is concerned, alkyl halides are known to be subject to photolysis and oxidation reactions in the atmosphere. The preference of alkyl halides for interfacial hydration opens up the possibility for their heterogeneous atmospheric processing at the surface of aerosols and other dispersed droplets. Previous studies have also shown that atmospheric oxidants, including the OH and HO_2 radicals, prefer the air–water interface [56, 57, 61, 92]. The partial hydration of alkyl halides at the aqueous surface (together with the interfacial presence of the oxidizing agent) will potentially affect the heterogeneous photolysis and oxidation reaction rates at the atmospheric aqueous surfaces in contrast to the gas phase or species fully solvated within the bulk liquid phase [67, 93, 94].

Unlike in the homogeneous-phase reactions, one of the important aspects of heterogeneous processes affecting their mechanisms and reaction rates is the alignment of reactants due to the orienting effect of the interface. For alkyl halides, the interfacial orientation is a result of a subtle balance of electrostatic, dispersion, induction and hydrogen-bonded interactions. Previous MD simulations showed interesting differences between the smallest molecules of the series, methyl halides (MeX), oriented preferentially with the CH_3 group into water and the halogen atom into the gas phase, and the molecules with 4- or 5-carbon chain, oriented parallel to the interface with the flexible nonpolar alkyl chain pointing on average slightly away from water [53, 54]. The present study reveals the details of the molecular orientation and the corresponding hydration at the water–vapor interface along the whole alkyl halide series. In particular, it shows that (a) the change in orientation from the alkyl chain (terminal methyl group) toward water to the alkyl chain (terminal methyl

group) away from water occurs gradually within the alkyl halide series, (b) the methyl halide molecules have their (incomplete) hydration shell centered on the methyl end of the molecule, while the hydration shell of the 2- to 5-carbon chain molecules is localized around the CH_2 group immediately next to the halogen, and (c) not only the methyl species, but also the ethyl and propyl halides have the halogen atom exposed, pointing essentially freely into the gas phase. Only as the length of the hydrophobic alkyl chain increases substantially beyond the polar region of the CH_2X group (i.e., for the 4- and 5-carbon chain), the halogen atom becomes more hydrated. The present MD simulations thus corroborate the conclusions of the previous studies carried out for only a few selected alkyl chlorides and bromides [53, 54], and show similar behavior also for alkyl iodides. The identity of the halogen substituent plays relatively minor role in the above general trend.

Ab initio studies [43, 44, 54, 70] have shown that the key factor for the alkyl halide hydration is a simultaneous occurrence of $X\cdots H_2O$ and $CH\cdots OH_2$ hydrogen bonds, with the hydrogen atoms of the α-CH_2 group (or, in the case of methyl halides, the CH_3 group) having the most positive electrostatic potential and being the preferential site for hydrogen bonding. In all alkyl halides, the region around the halogen atom possesses the most negative electrostatic potential, indicating its ability to act as proton acceptor. In methyl chloride, however, this negative region was shown to be less pronounced compared to pentyl chloride. Consequently, the $X\cdots H_2O$ hydrogen bonds of methyl chloride at the liquid water surface were found to be weaker and less frequent than the $CH\cdots OH_2$ bonds of the CH_3 group to the interfacial water molecules [54]. The character of the molecular electrostatic potential of alkyl halides and the resulting hydrogen-bonding patterns, as obtained from ab initio studies, thus provide rationalization of the orientational preferences of alkyl halides at the water–vapor interface predicted by MD simulations. Further ab initio investigations of a more complete set of alkyl halides, including the brominated and iodinated compounds, are needed to better understand their molecular properties and the nature of their interaction with water, as well as to test the adequacy of the present empirical model. The fact that the force field employed in the current MD simulations reproduces correctly the ab initio-based results for alkyl chlorides strongly suggests that the model is able to reliably describe, at least qualitatively, the interfacial hydration also for alkyl bromides and iodides.

As discussed above, the propensity of alkyl halides for interfacial solvation and the asymmetric hydration due to a particular molecular orientation is important for reactions of these compounds at aqueous atmospheric interfaces (on aerosols, cloud and fog droplets, and also on thin films of water on solid surfaces, on ice and snow). The differences in preferential orientation of the small alkyl halides versus the longer-chain ones relative to the aqueous surface are likely to have consequences for example in photochemical processes, in which caging by the solvent molecules plays a crucial role. The cage effect can be reduced at the water–vapor interface as a result of a less complete hydration shell of the interfacial species [65]. The present study shows that as the length of the alkyl chain increases, the halogen atom becomes increasingly (albeit still partially) hydrated. This indicates that partial caging of the halogen fragment upon photolysis of the C–X bond may occur for the longer-chain alkyl halides. For the small alkyl halides, however, such caging will be absent or substantially limited, as the short-chain compounds, when adsorbed at the water surface, tend to have the halogen atom exposed, with the C–X bond pointing into the gas phase. This concerns methyl, ethyl and propyl halides, which are the most atmospherically relevant ones, and thus suggests that the release of the reactive halogen radicals from photolysis of alkyl halides may be essentially unaffected by the interaction of alkyl halides with aqueous aerosols and other liquid droplets dispersed in air compared to the photochemical processing in the gas phase. While experimental studies of interfacial processes with sensitivity to molecular alignment remain challenging at ambient conditions, more information on the uptake and photochemistry of alkyl halides on aqueous surfaces may be obtained from molecular beam experiment with water clusters [95–97]. These experiments, employing the pickup technique, have been performed for a range of atmospherically relevant molecules (e.g., HCl, HBr, CH_3OH and CH_3CH_2OH) [96] and should thus be feasible also for the short-chain alkyl halides. In addition to providing validation of our theoretical predictions made on the basis of a computational model, such experiments would be valuable in regards to the reactivity of low molecular weight alkyl halides on atmospheric ice particles, which is important from the point of view of the ozone layer depletion in polar regions.

Finally, we note that adsorption behavior of alkyl halides can be significantly influenced by organics present at the interface. In many environments, field studies have shown that a major fraction of aqueous aerosol particles as well as fog and rain droplets comprises a variety of surface-active organic material, from long chain fatty acids [98] to shorter chain compounds [99] to complex humic-like substances [100]. Depending on the type of surfactant and its surface coverage, interfacial partitioning, residence times and orientation of alkyl halides at the surfactant-coated aqueous or ice surfaces may be different than those at the neat air–water or air–ice interfaces [101, 102]. Further work is needed to bring insight into how the presence of surfactants will affect the interfacial behavior of alkyl halides.

5 Conclusions

Adsorption of gas-phase *n*-alkyl halides to the surface of a liquid water slab and their hydration at the water–vapor interface were studied using classical MD simulations. The investigated alkyl halide species included monosubstituted methyl to pentyl halides, R–X, where X = Cl, Br, or I, and R = C_nH_{2n+1}, n = 1–5. Our results show that all of the alkyl halides have a strong tendency to reside at the water–vapor interface, in accord with the findings of previous studies for a few selected chloro- and bromoalkanes [53–55] as well as other small organics and gases [56–59, 61, 85]. This phenomenon may result in considerable adsorption or even accumulation of alkyl halides at the air–water interface, although the low molecular weight alkyl halides investigated here are rather volatile and, at the same time, are not viewed as particularly "surface active."

The present MD study reveals the details of the molecular orientation and the corresponding hydration at the water–vapor interface for the alkyl halide series. In particular, it shows that all methyl halide molecules, including methyl iodide which has not been previously studied, have their (incomplete) hydration shell centered on the methyl end of the molecule, while the halogen atom is facing the gas phase essentially unsolvated. The hydration shell of the 2- to 5-carbon chain molecules is localized around the α-CH_2 group next to the halogen, in accord with ab initio results for pentyl chloride [54]. However, ethyl and, to a large degree, also propyl halides, with their relatively short alkyl chain, still have the halogen atom rather exposed, pointing almost freely into the gas phase. The behavior of butyl and pentyl halides on the water surface begins to resemble that of alcohols, with the polar region of the CH_2X group interacting with water and the rest of the increasingly nonpolar hydrocarbon chain pointing on average away from water. Consequently, the halogen atom becomes more, albeit not fully, hydrated. The identity of the halogen substituent plays only a minor role in this general trend.

The above findings regarding the solvation behavior of alkyl halides at the water–vapor interface have possible important consequences for atmospheric chemistry. In systems with large air–water interface area, such as the aqueous aerosols and other airborne liquid droplets, the propensity of alkyl halides for the water–vapor interface may result in significant enhancement of their surface concentrations. While the importance of interfacial adsorption of haloalkanes has been demonstrated experimentally in the field of water treatment for air bubbles dispersed in water [89–91], uptake and heterogeneous atmospheric processing on the surface of aqueous aerosol and cloud droplets has not received much attention so far. Our results show that the interfacial partitioning of alkyl halides may need to be taken into account when interpreting the results of field studies or laboratory experiments involving the aerosol phase. In addition, the partitioning of alkyl halides to the aqueous aerosol surfaces should be considered in tropospheric models. At the same time, the specific character of the partial hydration of the surface-adsorbed alkyl halides is likely to affect the reactivity of these species when adsorbed on the surface of aqueous or ice particles in the atmosphere. The distinct difference in preferred alignment and solvation structures at the aqueous surface between the short-chain alkyl halides and their longer-chain counterparts is of potential importance particularly for heterogeneous photochemistry of alkyl halides on atmospheric aqueous and/or ice interfaces. Experimental investigation of such systems and processes, for example in molecular beam experiments with the pickup and photodissociation of alkyl halides on water clusters, would be of high relevance for atmospheric science.

Acknowledgments The authors wish to thank Jan Heyda for technical assistance with the computations of the spatial distribution functions. The research in Prague was supported by the Czech Science Foundation Grant no. P208/10/1724 and by RVO 61388963. B.M. would like to acknowledge financial support from the Czech Science Foundation (Grant no. 13-08651S). A.H. acknowledges the support from SVV265304. Support to A.O. and M.R. via the KONTAKT program of the Ministry of Education, Youth and Sports of the Czech Republic (Grant ME09064), and to M.R. by the AirUCI Institute funded by the U.S. National Science Foundation (Grant no. 0909227) is also gratefully appreciated. Part of the work has been carried out by A.O. as a student research project at an international summer school Schola Ludus 2009 in Nove Hrady (http://auc.cz/scholaludus), which received financial support from the European Social Fund and from the government of the Czech Republic.

References

1. Finlayson-Pitts BJ, Pitts JN Jr (2000) Chemistry of the upper and lower atmosphere: theory, experiments, and applications. Academic Press, San Diego
2. Carpenter LJ (2003) Iodine in the marine boundary layer. Chem Rev 103(12):4953–4962. doi:10.1021/cr0206465
3. Barrie LA, Bottenheim JW, Schnell RC, Crutzen PJ, Rasmussen RA (1988) Ozone destruction and photochemical reactions at polar sunrise in the lower Arctic atmosphere. Nature 334:138–141
4. Keene WC, Khalil MAK, Erickson DJ, McCulloch A, Graedel TE, Lobert JM, Aucott ML, Gong SL, Harper DB, Kleiman G, Midgley P, Moore RM, Seuzaret C, Sturges WT, Benkovitz CM, Koropalov V, Barrie LA, Li YF (1999) Composite global emissions of reactive chlorine from anthropogenic and natural sources: reactive Chlorine Emissions Inventory. J Geophys Res Atmos 104(D7):8429–8440. doi:10.1029/1998jd100084
5. Lovelock JE (1975) Natural halocarbons in air and in sea. Nature 256:193–194
6. Khalil MAK, Moore RM, Harper DB, Lobert JM, Erickson DJ, Koropalov V, Sturges WT, Keene WC (1999) Natural emissions of chlorine-containing gases: reactive chlorine emissions inventory. J Geophys Res Atmos 104(D7):8333–8346. doi:10.1029/1998jd100079

7. Greenberg JP, Guenther AB, Turnipseed A (2005) Marine organic halide and isoprene emissions near Mace Head, Ireland. Environ Chem 2:291–294
8. Bill M, Rhew RC, Weiss RF, Goldstein AH (2002) Carbon isotope ratios of methyl bromide and methyl chloride emitted from a coastal salt marsh. Geophys Res Lett 29:4/1–4/4
9. Rhew RC, Miller BR, Weiss RF (2000) Natural methyl bromide and methyl chloride emissions from coastal salt marshes. Nature 403:292–295
10. Yokouchi Y, Noljiri Y, Barrle LA, Toom-Sauntry D, Machlda T, Inuzuka Y, Aklmoto H, Li HJ, Fujinuma Y, Aoki S (2000) A strong source of methyl chloride to the atmosphere from tropical coastal land. Nature 403:295–298
11. Crutzen PJ, Heidt LE, Krasnec JP, Pollock WH, Seiler W (1979) Biomass burning as a source of atmospheric gases CO, H_2, N_2O, NO, CH_3Cl and COS. Nature 282:253–256
12. Keppler F, Eiden R, Niedan V, Pracht J, Scholer HF (2000) Halocarbons produced by natural oxidation processes during degradation of organic matter. Nature 403:298–301
13. Rasmussen RA, Rasmussen LE, Khalil MAK, Dalluge RW (1980) Concentration distribution of methyl chloride in the atmosphere. J Geophys Res Oceans 85(C12):7350–7356. doi:10.1029/JC085iC12p07350
14. Low JC, Wang NY, Williams J, Cicerone RJ (2003) Measurements of ambient atmospheric C_2H_5Cl and other ethyl and methyl halides at coastal California sites and over the Pacific Ocean. J Geophys Res Atmos 108(D19):4608. doi:10.1029/2003JD003620
15. Yagi YL, Williams J, Wang N-Y, Cicerone RJ (1993) Agricultural soil fumigation as a source of atmospheric methyl bromide. Proc Natl Acad Sci 90:8420–8423
16. Yagi YL, Williams J, Wang N-Y, Cicerone RJ (1995) Atmospheric methyl bromide (CH_3Br) from agricultural soil fumigations. Science 267:1979–1981
17. Yates SR, Wang D, Ernst FF, Gan J (1997) Methyl bromide emissions from agricultural fields: bare soil, deep injection. Environ Sci Technol 31:1136–1143
18. Ristaino JB, Thomas W (1997) Agriculture, methyl bromide and the ozone hole. Can we fill the gaps? Plant Dis 81:964–977
19. Andreae MO, Atlas E, Harris GW, Helas G, de Kock A, Koppmann R, Maenhaut W, Mano S, Pollock WH, Rudolph J, Scharffe D, Schebeske G, Welling M (1996) Methyl halide emissions from savanna fires in southern Africa. J Geophys Res Atmos 101(D19):23603–23613. doi:10.1029/95JD01733
20. Thomas VM, Bedford JA, Cicerone RJ (1997) Bromine emissions from leaded gasoline. Geophys Res Lett 24:1371–1374
21. Thornton JA, Kercher JP, Riedel TP, Wagner NL, Cozic J, Holloway JS, Dube WP, Wolfe GM, Quinn PK, Middlebrook AM, Alexander B, Brown SS (2010) A large atomic chlorine source inferred from mid-continental reactive nitrogen chemistry. Nature 464:271–274
22. Graedel TE, Keene WC (1995) Tropospheric budget of reactive chlorine. Global Biogeochem Cycles 9:47–77
23. Carpenter LJ, Sturges WT, Penkett SA, Liss PS, Alicke B, Hebestreit K, Platt U (1999) Short-lived alkyl iodides and bromides at Mace Head, Ireland: links to biogenic sources and halogen oxide production. J Geophys Res Atmos 104(D1):1679–1689. doi:10.1029/98JD02746
24. Butler JH (2000) Atmospheric chemistry: better budgets for methyl halides? Nature 403:260–261
25. Platt U, Janssen C (1995) Observaton and role of the free radicals NO_3, ClO, BrO, and IO in the troposphere. Faraday Discuss 100:175–198
26. Sekusak S, Gusten H, Sablijic A (1995) An ab initio investigation on transition states and reactivity of chloroethane with OH radical. J Chem Phys 102:7504–7518
27. Mellouki A, Talukdar RK, Schmoltner A, Gierczak T, Mills MJ, Solomon S, Ravishankara AR (1992) Atmospheric lifetimes and ozone depletion potentials of methyl bromide and dibromomethane. Geophys Res Lett 19:2059–2062
28. Solomon S, Mills M, Heidt LE, Pollock WH, Tuck AF (1992) On the evaluation of ozone depletion potential. J Geophys Res Atmos 97(D1):825–842
29. Khalil MAK, Rasmussen RA (1999) Atmospheric methyl chloride. Atmos Environ 33:1305–1321
30. Yvon-Lewis SA, Saltzman ES, Montzka SA (2009) Recent trends in atmospheric methyl bromide: analysis of post-Montreal Protocol variability. Atmos Chem Phys 9:5963–5974
31. Yoshida Y, Wang Y, Shim C, Cunnold D, Blake DR, Dutton GS (2006) Inverse modeling of the global methyl chloride sources. J Geophys Res Atmos 111:D16307
32. Bell N, Hsu L, Jacob DJ, Schultz MG, Blake DR, Butler JH, King DB, Lobert JM, Maier-Reimer E (2002) Methyl iodide: atmospheric budget and use as a tracer of marine convection in global models. J Geophys Res Atmos 107(D17):4340
33. Molina MJ, Tso T-L, Molina LT, Wang FC-Y (1987) Antarctic stratospheric chemistry of chlorine nitrate, hydrogen chloride, and ice: release of active chlorine. Science 238:1253–1257
34. Grecea ML, Backus EHG, Kleyn AW, Bonn M (2005) Surface photochemistry of bromoform on ice: cross section and competing reaction pathways. J Phys Chem B 109(37):17574–17578. doi:10.1021/jp052586n
35. Finlayson-Pitts BJ (2009) Reactions at surfaces in the atmosphere: integration of experiments and theory as necessary (but not necessarily sufficient) for predicting the physical chemistry of aerosols. PCCP 11(36):7760–7779. doi:10.1039/b906540g
36. Pal SK, Mereshchenko AS, El-Khoury PZ, Tarnovsky AN (2011) Femtosecond photolysis of CH_2Br_2 in acetonitrile: capturing the bromomethyl radical and bromine-atom charge transfer complex through deep-to-near UV probing. Chem Phys Lett 507(1–3):69–73. doi:10.1016/j.cplett.2011.02.046
37. Zhu R, Tang B, Ji L, Tang Y, Zhang S, Zhang B (2004) Photodissociation dynamics of n-alkyl bromide at 234 and 267 nm. Opt Commun 235(4–6):325–331. doi:10.1016/j.optcom.2004.02.055
38. Karras G, Danakas S, Kosmidis C (2011) Formation of molecular halide ions from alkyl-halide clusters irradiated by ps and fs laser pulses. J Phys Chem A 115(17):4186–4194. doi:10.1021/jp2015947
39. Miranda MA, Pérez-Prieto J, Font-Sanchis E, Scaiano JC (2001) One- vs two-photon processes in the photochemistry of 1, n-dihaloalkanes. Acc Chem Res 34(9):717–726. doi:10.1021/ar000107r
40. Preston TJ, Dutta M, Esselman BJ, Kalume A, George L, McMahon RJ, Reid SA, Crim FF (2011) Formation and relaxation dynamics of iso-CH_2Cl–I in cryogenic matrices. J Chem Phys 135(11):114503–114510
41. Lilach Y, Asscher M (2003) Photochemistry of caged molecules: CD_3Cl@Ice. J Chem Phys 119(1):407–412
42. Ayoub Y, Asscher M (2008) Photochemistry of ethyl chloride caged in amorphous solid water. Phys Chem Chem Phys 10(43):6486–6491
43. Dozova N, Krim L, Alikhani ME, Lacome N (2005) Vibrational spectra and structure of CH_3Cl:H_2O, CH_3Cl:HDO, and CH_3Cl:D_2O complexes. IR matrix isolation and ab initio calculations. J Phys Chem A 109(45):10273–10279. doi:10.1021/jp053895g
44. Dozova N, Krim L, Alikhani ME, Lacome N (2007) Vibrational spectra and structure of CH_3Cl:$(H_2O)_2$ and CH_3Cl:$(D_2O)_2$ complexes. IR matrix isolation and ab initio calculations. J Phys Chem A 111(40):10055–10061. doi:10.1021/jp074028
45. Aida M, Yamataka H, Dupuis M (1998) Ab initio molecular dynamics simulations on the hydrolysis of methyl chloride with

explicit consideration of three water molecules. Chem Phys Lett 292(4–6):474–480. doi:10.1016/S0009-2614(98)00706-4
46. Aida M, Yamataka H, Dupuis M (1999) Ab initio MD simulations of a prototype of methyl chloride hydrolysis with explicit consideration of three water molecules: a comparison of MD trajectories with the IRC path. Theor Chem Acc 102(1–6):262–271. doi:10.1007/s002140050497
47. Fournier F, Dubost H, Carrez S, Zheng W, Bourguignon B (2005) Interaction of coadsorbed CH_3Cl and D_2O layers on Pd(111) studied by sum frequency generation. J Chem Phys 123(18):184705–184707
48. Vaida ME, Bernhardt TM (2012) Surface-aligned femtochemistry: photoinduced reaction dynamics of CH_3I and CH_3Br on MgO(100). Faraday Discuss 157:437–449
49. DeSimone AJ, Olanrewaju BO, Grieves GA, Orlando TM (2013) Photodissociation of methyl iodide adsorbed on low-temperature amorphous ice surfaces. J Chem Phys 138(8): 084703–084709
50. Berger R, Lilach Y, Ayoub Y, Asscher M (2005) Photochemistry of molecules at confined environment: CD_3Br/O/Ru(001) and CO_2 @ Ice. Isr J Chem 45(1–2):97–109. doi:10.1560/veyg-4lq8-dtpt-tdu4
51. Swanson AL, Blake NJ, Blake DR, Sherwood Rowland F, Dibb JE, Lefer BL, Atlas E (2007) Are methyl halides produced on all ice surfaces? Observations from snow-laden field sites. Atmos Environ 41(24):5162–5177. doi:10.1016/j.atmosenv.2006.11.064
52. Swanson AL, Blake NJ, Dibb JE, Albert MR, Blake DR, Sherwood Rowland F (2002) Photochemically induced production of CH_3Br, CH_3I, C_2H_5I, ethene, and propene within surface snow at Summit, Greenland. Atmos Environ 36(15–16):2671–2682. doi:10.1016/S1352-2310(02)00127-9
53. Harper K, Minofar B, Sierra-Hernandez MR, Casillas-Ituarte NN, Roeselova M, Allen HC (2009) Surface residence and uptake of methyl chloride and methyl alcohol at the air/water interface studied by vibrational sum frequency spectroscopy and molecular dynamics. J Phys Chem A 113:2015–2024
54. Pasalic H, Roeselova M, Lischka H (2011) Methyl and pentyl chloride in a microhydrated environment and at the liquid water-vapor interface: a theoretical study. J Phys Chem B 115: 1807–1816
55. Habartová A, Valsaraj KT, Roeselová M (2013) Molecular dynamics simulations of small halogenated organics at the air-water interface: implications in water treatment and atmospheric chemistry. J Phys Chem A. doi:10.1021/jp405292k
56. Vieceli J, Roeselova M, Potter N, Dang LX, Garrett BC, Tobias DJ (2005) Molecular dynamics simulations of atmospheric oxidants at the air-water interface: solvation and accommodation of OH and O_3. J Phys Chem B 109(33):15876–15892. doi:10.1021/jp051361
57. Vacha R, Slavicek P, Mucha M, Finlayson-Pitts BJ, Jungwirth P (2004) Adsorption of atmospherically relevant gases at the air/water interface: free energy profiles of aqueous solvation of N_2, O_2, O_3, OH, H_2O, HO_2, and H_2O_2. J Phys Chem A 108: 11573–11579
58. Vacha R, Jungwirth P, Chen J, Valsaraj KT (2006) Adsorption of polycyclic aromatic hydrocarbons at the air-water interface: molecular dynamics simulations and experimental atmospheric observations. PCCP 8(38):4461–4467. doi:10.1039/b610253k
59. Liyana-Arachchi TP, Valsaraj KT, Hung FR (2011) Molecular simulation study of the adsorption of naphthalene and ozone on atmospheric air/ice interfaces. J Phys Chem A 115(33): 9226–9236. doi:10.1021/jp205246z
60. Hub JS, Caleman C, van der Spoel D (2012) Organic molecules on the surface of water droplets: an energetic perspective. PCCP 14:9537–9545. doi:10.1039/c2cp40483d
61. Roeselova M, Vieceli J, Dang LX, Garrett BC, Tobias DJ (2004) Hydroxyl radical at the air-water interface. J Am Chem Soc 126(50):16308–16309. doi:10.1021/ja045552m
62. Harrison I, Polanyi JC, Young PA (1988) Photochemistry of adsorbed molecules. 3.Photodissociation and photodesorption of CH3Br adsorbed on LiF(001). J Chem Phys 89(3):1475–1497. doi:10.1063/1.455148
63. Slavicek P, Roeselova M, Jungwirth P, Schmidt B (2001) Preference of cluster isomers as a result of quantum delocalization: potential energy surfaces and intermolecular vibrational states of Ne···HBr, Ne···HI, and $HI(Ar)_n$ ($n = 1 - 6$). J Chem Phys 114(4):1539–1548
64. Rieley H, McMurray DP, Haq S (1996) Adsorption and photochemistry of dinitrogen tetroxide on low temperature ice layers. J Chem Soc Faraday Trans 92(6):933–939. doi:10.1039/ft9969200933
65. Donaldson DJ, Valsaraj KT (2009) Adsorption and reaction of trace gas-phase organic compounds on atmospheric water film surfaces: a critical review. Environ Sci Technol 44:865–873
66. Wingen LM, Moskun AC, Johnson SN, Thomas JL, Roeselova M, Tobias DJ, Kleinman MT, Finlayson-Pitts BJ (2008) Enhanced surface photochemistry in chloride-nitrate ion mixtures. PCCP 10(37):5668–5677. doi:10.1039/b806613b
67. Nissenson P, Knox CJH, Finlayson-Pitts BJ, Phillips LF, Dabdub D (2006) Enhanced photolysis in aerosols: evidence for important surface effects. PCCP 8(40):4700–4710. doi:10.1039/B609219e
68. Case DA, Darden TA, Cheatham TEI, Simmerling CL, Wang J, Duke RE, Luo R, Merz KM, Wang B, Pearlman DA, Crowley M, Brozell S, Tsui V, Gohlke H, Mongan J, Hornak V, Cui G, Beroza P, Schafmeister C, Caldwell JW, Ross WR, Kollman PA (2004) AMBER 8. University of California, San Francisco
69. Dang LX (1992) The nonadditive intermolecular potential for water revised. J Chem Phys 97:2659–2660
70. Wang W, Tian A, Wong N-B (2005) Theoretical study on the bromomethane-water 1:2 complexes. J Phys Chem A 109: 8035–8040
71. Frisch MJ, Trucks GW, Schlegel HB, Scuseria GE, Robb MA, Cheeseman JR, Montgomery JA, Jr, Vreven T, Kudin KN, Burant JC, Millam JM, Iyengar SS, Tomasi J, Barone V, Mennucci B, Cossi M, Scalmani G, Rega N, Petersson GA, Nakatsuji H, Hada M, Ehara M, Toyota K, Fukuda R, Hasegawa J, Ishida M, Nakajima T, Honda Y, Kitao O, Nakai H, Klene M, Li X, Knox JE, Hratchian HP, Cross JB, Bakken V, Adamo C, Jaramillo J, Gomperts R, Stratmann RE, Yazyev O, Austin AJ, Cammi R, Pomelli C, Ochterski JW, Ayala PY, Morokuma K, Voth GA, Salvador P, Dannenberg JJ, Zakrzewski VG, Dapprich S, Daniels AD, Strain MC, Farkas O, Malick DK, Rabuck AD, Raghavachari K, Foresman JB, Ortiz JV, Cui Q, Baboul AG, Clifford S, Cioslowski J, Stefanov BB, Liu G, Liashenko A, Piskorz P, Komaromi I, Martin RL, Fox DJ, Keith T, Al-Laham MA, Peng CY, Nanayakkara A, Challacombe M, Gill PMW, Johnson B, Chen W, Wong MW, Gonzalez C, Pople JA (2004) Gaussian 03, Revision D.01. Gaussian, Inc., Wallingford, CT
72. Hirose C, Akamatsu N, Domen K (1992) Formulas for the analysis of surface sum-frequency generation spectrum by CH stretching modes of methyl and methylene groups. J Chem Phys 96:997–1004
73. Feller D (1996) The role of databases in support of computational chemistry calculations. J Comput Chem 17:1571–1586
74. Schuchardt KL, Didier BT, Elsethagen TO, Sun L, Gurumoorthi V, Chase JM, Li J, Windus TL (2007) Basis set exchange: a community database for computational sciences. J Chem Inf Model 47(3):1045–1052. doi:10.1021/ci600510j

75. Bayly CI, Cieplak P, Cornell WD, Kollman PA (1993) A well-behaved electrostatical potential based method using charge restraints for deriving atomic charges: the RESP model. J Phys Chem 97(40):10269–10280. doi:10.1021/j100142a004
76. Wang J, Wang W, Kollman PA, Case DA (2006) Automatic atom type and bond type perception in molecular mechanical calculations. J Mol Graph Modell 25:247–260
77. Case DA, Darden TA, Cheatham TE, Simmerling CL, Wang J, Duke RE, Luo R, Walker RC, Zhang W, Merz KM, Roberts B, Wang B, Hayik S, Roitberg A, Seabra G, Kolossvary I, Wong KF, Paesani F, Vanicek J, Liu J, Wu X, Brozell SR, Steinbrecker T, Gohlke H, Cai Q, Ye X, Wang J, Hsieh M-J, Cui G, Roe DR, Mathews DH, Seetin MG, Sagui C, Babin V, Luchko T, Gusarov S, Kovalenko A, Kollman PA (2010) AMBER 11. University of California, San Francisco
78. Berendsen HJC, Postma JPM, van Gunsteren WF, DiNola A, Haak JR (1984) Molecular dynamics with coupling to an external bath. J Chem Phys 81:3684–3690
79. Hockney RW, Goel SP, Eastwood JW (1974) Quiet high-resolution computer models of a plasma. J Comput Phys 14(2): 148–158
80. Darden T, York D, Pedersen LG (1993) Particle mesh Ewald: an N.Log(N) method for Ewald sums in large systems. J Chem Phys 98(12):10089–10092
81. Essmann U, Perera L, Berkowitz ML, Darden T, Lee H, Pedersen LG (1995) A smooth particle mesh Ewald method. J Chem Phys 103(null):8577–8593
82. Ryckaert JP, Ciccotti G, Berendsen HJC (1977) Numerical integration of the cartesian equations of motion of a system with constraints: molecular dynamics of n-alkanes. J Comput Phys 23:327–341
83. Miyamoto S, Kollman PA (1992) SETTLE: an analytical version of the SHAKE and RATTLE algorithm for rigid water models. J Comput Chem 13:952–962
84. Humphrey W, Dalke A, Schulten K (1996) VMD: visual molecular dynamics. J Molec Graph 14:33–38
85. Murdachaew G, Varner ME, Phillips LF, Finlayson-Pitts BJ, Gerber RB (2013) Nitrogen dioxide at the air-water interface: trapping, absorption, and solvation in the bulk and at the surface. PCCP 15(1):204–212. doi:10.1039/c2cp42810e
86. Lide DR (ed) (2007-2008) Aqueous solubility of organic compounds. In CRC Handbook of Chemistry and Physics, 88th ed. Taylor and Francis, Boca Raton, FL
87. Sander R (1999) Compilation of Henry's law constants for inorganic and organic species of potential importance in environmental chemistry. http://www.henrys-law.org
88. Vrbka L, Mucha M, Minofar B, Jungwirth P, Brown EC, Tobias DJ (2004) Propensity of soft ions for the air/water interface. Curr Opin Colloid Interface Sci 9(1–2):67–73. doi:10.1016/j.cocis.2004.05.028
89. Smith JS, Burns LF, Valsaraj KT, Thibodeaux LJ (1996) Bubble column reactors for wastewater treatment. 2. The effect of sparger design on sublation column hydrodynamics in the homogeneous flow regime. Ind Eng Chem Res 35(5): 1700–1710. doi:10.1021/ie950366y
90. Smith JS, Valsaraj KT (1997) Bubble column reactors for wastewater treatment. 3. Pilot-scale solvent sublation of pyrene and pentachlorophenol from simulated wastewater. Ind Eng Chem Res 36(3):903–914. doi:10.1021/ie9605241
91. Smith JS, Valsaraj KT, Thibodeaux LJ (1996) Bubble column reactors for wastewater treatment.1. Theory and modeling of continuous countercurrent solvent sublation. Ind Eng Chem Res 35(5):1688–1699. doi:10.1021/ie9503656
92. Morita A, Kanaya Y, Francisco JS (2003) Uptake of HO_2 radical by water: molecular dynamics calculations and their implications for atmospheric modeling. J Geophys Res 109:Article No. D09210
93. Valsaraj KT (2009) Trace gas adsorption thermodynamics at the air-water interface: implications in atmospheric chemistry. Pure Appl Chem 81(10):1889–1901. doi:10.1351/pac-con-08-07-06
94. Watanabe H, Yamaguchi S, Sen S, Morita A, Tahara T (2010) "Half-hydration" at the air/water interface revealed by heterodyne-detected electronic sum frequency generation spectroscopy, polarization second harmonic generation, and molecular dynamics simulation. J Chem Phys 132(14):144701
95. Poterya V, Farnik M, Slavicek P, Buck U, Kresin VV (2007) Photodissociation of hydrogen halide molecules on free ice nanoparticles. J Chem Phys 126(7). doi:10.1063/1.2709635
96. Lengyel J, Kocisek J, Poterya V, Pysanenko A, Svrckova P, Farnik M, Zaouris DK, Fedor J (2012) Uptake of atmospheric molecules by ice nanoparticles: pickup cross sections. J Chem Phys 137(3). doi:10.1063/1.4733987
97. Pradzynski CC, Forck RM, Zeuch T, Slavicek P, Buck U (2012) A fully size-resolved perspective on the crystallization of water clusters. Science 337(6101):1529–1532. doi:10.1126/science.1225468
98. Tervahattu T, Juhanoja J, Vaida V, Tuck AF, Niemi JV, Kupiainen K, Kulmala M, Vehkamäki H (2005) Fatty acids on continental sulfate aerosol particles. J Geophys Res 110:D06207
99. Russell LM, Maria SF, Myneni SCB (2002) Mapping organic coatings on atmospheric particles. Geophys Res Lett 29. 10.1029/2002GL014874
100. Raja S, Raghunathan R, Yu XY, Lee TY, Chen J, Kommalapati RR, Murugesan K, Shen X, Qingzhong Y, Valsaraj KT, Collett JL (2008) Fog chemistry in the Texas-Louisiana gulf coast corridor. Atmos Environ 42:2048
101. Liyana-Arachchi TP, Valsaraj KT, Hung FR (2012) Adsorption of naphthalene and ozone on atmospheric air/ice interfaces coated with surfactants: a molecular simulation study. J Phys Chem A 116(10):2519–2528. doi:10.1021/jp3002417
102. Wick CD, Chen B, Valsaraj KT (2010) Computational investigation of the influence of surfactants on the air-water interfacial behavior of polycylic aromatic hydrocarbons. J Phys Chem C 114(34):14520–14527. doi:10.1021/jp1039578